

Ab Initio IGLO Study of the φ - and ψ -Angle Dependence of the ^{13}C Chemical Shifts in the Model Peptide *N*-Acetyl-*N'*-methylglycinamide

Ding Jiao, Michael Barfield,* and Victor J. Hruby

Contribution from the Department of Chemistry, University of Arizona, Tucson, Arizona 85721

Received May 24, 1993*

Abstract: The ab initio IGLO (individual gauge for localized orbitals) method was used to examine the conformational dependencies of the isotropic ^{13}C chemical shifts in the model peptide *N*-acetyl-*N'*-methylglycinamide. A surface plot of the calculated ^{13}C isotropic chemical shifts for the $\text{C}\alpha$ carbon was constructed at 30° grid intervals of the φ and ψ angles. These data are used to examine the relationship between chemical shifts and protein secondary structure. The $\text{C}\alpha$ carbons in α -helix and β -sheet conformations are calculated to be shifted 2.3 ppm downfield and 2.9 ppm to high field, respectively, of the random coil value. Considering the spread in experimental values, especially for the β -sheet conformations, these secondary shifts are in reasonable agreement with the average experimental values of 3.2 and -1.2 ppm, respectively, for glycol residues in peptides and proteins. The smaller differences predicted for other types of secondary structures are also consistent with the experimental results. Thus, for the $\text{C}\alpha$ carbon it is not necessary to include interresidue hydrogen-bonding effects to explain the major chemical shift trends. An analysis of the localized MO contributions (LMOC) shows that all four bonds directly connected to the $\text{C}\alpha$ carbon are important to the total shift but each of these has a different (φ, ψ) angle dependence. The LMOC from the $\text{C}\alpha$ - C' bond provides the largest contribution to the chemical shift difference between the α -helix and the β -sheet conformations.

I. Introduction

In peptides and proteins, the sensitivity of the ^{13}C chemical shifts to conformational variations is well-known.¹⁻³ With improved isotopic substitution strategies⁴ and new methodologies in heteronuclear multidimensional NMR,⁵ two groups have recently reported statistical correlations of the ^{13}C chemical shifts with the secondary structures of proteins.^{6,7} A strong correlation was noted between the $\text{C}\alpha$ chemical shift and the secondary structure, especially α -helix and β -sheet; i.e., the $\text{C}\alpha$ resonances for α -helix structures are at higher frequency (lower field) than in β -sheet conformations. Similar correlations also were found for carbonyl and side-chain $\text{C}\beta$ carbons. Typical patterns in the observed chemical shifts for backbone and side-chain carbons are shown in Figure 1. Tonelli⁸ attempted to rationalize the experimental ^{13}C chemical shifts for $\text{C}\beta$ and $\text{C}=\text{O}$ carbons on the basis of empirical substituent effects, particularly the gauche/anti dependence of the γ -effects.^{9,10} The α -carbon chemical shifts were not discussed.

Ando and co-workers^{11,12} used semiempirical MO methods to investigate the (φ, ψ) angle shift dependency of the model dipeptide *N*-acetyl-*N'*-methyl-*L*-alaninamide. They proposed that the ^{13}C chemical shifts are sensitive to changes in the electronic distri-

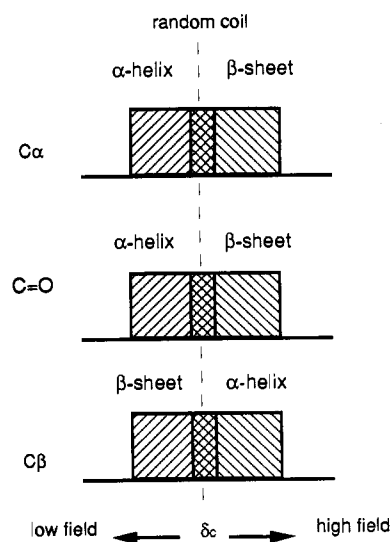


Figure 1. Schematic representation of the experimental ^{13}C chemical shifts of $\text{C}\alpha$, $\text{C}=\text{O}$, and $\text{C}\beta$ in peptides and proteins.

butions with (φ, ψ) angle changes as well as to the effect of intra- and/or interresidue hydrogen bonds. However, the semiempirical results did not provide an adequate description of the $\text{C}\alpha$ chemical shifts. For ^{13}C chemical shifts the effects of interresidue hydrogen bonding are expected to be more important for $\text{C}=\text{O}$ groups¹³ than for the $\text{C}\alpha$ carbon, which is not directly involved in hydrogen bonding. More recently, ab initio methods have been used to show that $\text{C}\alpha$ and $\text{C}\beta$ shifts in alanine residues are largely determined by the (φ, ψ) angle dependence.¹⁴

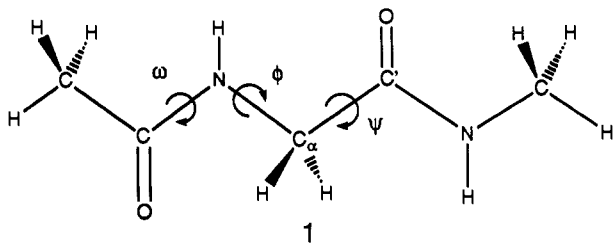
Distributed-origins methods¹⁵ such as IGLO¹⁶ have been used extensively for ab initio shielding computations. Studies from these laboratories have emphasized the conformational and

- * Abstract published in *Advance ACS Abstracts*, October 15, 1993.
 (1) Breitmaier, E.; Voelter, W. *Carbon-13 NMR Spectroscopy, High-Resolution Methods and Applications in Organic Chemistry and Biochemistry*, 3rd ed.; Heyden: New York, 1987.
 (2) Tonelli, A. E.; Schilling, F. C. *Acc. Chem. Res.* **1981**, *14*, 233–238.
 (3) For a review, see: Saitō, H. *Magn. Reson. Chem.* **1986**, *24*, 835–852.
 (4) LeMaster, D. M.; Richards, F. M. *Biochemistry* **1988**, *27*, 142–150.
 (5) Ikura, M.; Kay, L. E.; Bax, A. *Biochemistry* **1990**, *29*, 4659–4667.
 (6) Spera, S.; Bax, A. *J. Am. Chem. Soc.* **1991**, *113*, 5490–5492.
 (7) Wishart, D. S.; Sykes, B. D.; Richards, F. M. *J. Mol. Biol.* **1991**, *222*, 311–333.
 (8) (a) Tonelli, A. E. *J. Am. Chem. Soc.* **1980**, *102*, 7635–7637. (b) Tonelli, A. E. *Biopolymers* **1984**, *23*, 819–829.
 (9) Grant, D. M.; Paul, E. G. *J. Am. Chem. Soc.* **1964**, *86*, 2984–2990.
 (10) Grant, D. M.; Cheney, B. V. *J. Am. Chem. Soc.* **1967**, *89*, 5315–5318.
 Woolfenden, W. R.; Grant, D. M. *J. Am. Chem. Soc.* **1966**, *88*, 1496–1502.
 (11) Ando, I.; Saitō, H.; Tabeta, R.; Shoji, A.; Ozaki, T. *Macromolecules* **1984**, *17*, 457–461.
 (12) (a) Ando, S.; Ando, I.; Shoji, A.; Ozaki, T. *J. Am. Chem. Soc.* **1988**, *110*, 3380–3386. (b) Asakawa, N.; Kuroki, S.; Kurosu, H.; Ando, I.; Shoji, A.; Ozaki, T. *J. Am. Chem. Soc.* **1992**, *114*, 3261–3265.

(13) Chesnut, D. B.; Phung, C. G. In *NMR Shieldings and Molecular Structure*; Tossell, J. A., Ed.; Kluwer Academic Publishers: Norwell, MA, 1993; pp 221–241.

(14) de Dios, A. C.; Pearson, J. G.; Oldfield, E. *Science* **1993**, *260*, 1491–1495.

substituent dependencies of ^{13}C chemical shifts in organic and biochemical molecules.^{17–21} In most cases the experimental conformational ^{13}C chemical shift trends are reproduced even with relatively small basis sets. Presented here is an ab initio IGLO study of the conformational dependence of ^{13}C chemical shifts in *N*-acetyl-*N'*-methylglycinamide (1). The glycine dipep-



ptide is chosen as a model compound for two reasons. Glycine is the smallest among the 20 natural amino acids, and it is unique in its lack of chirality at C_α. Since the energy contour has a C₂ symmetry axis through $\phi = 0^\circ$, $\psi = 0^\circ$,²² the computational effort required for both geometry optimizations and shielding calculations is reduced. The conformational dependencies of C_α chemical shifts have been observed for nearly all the amino acids, including Gly residues.^{6,7} Because they exhibit similar trends in α -helix and β -sheet conformations, a common electronic origin is expected, and the Gly dipeptide should provide a simple model for the observed conformational dependence of C_α chemical shifts. This model does not include β -carbons or the effects of interresidue hydrogen bonding.

II. Computational Methods

Because of the sensitivity of chemical shielding to molecular geometries^{23,24} and the unavailability of good experimental structural data, the usual procedure is to use the best energy-optimized structures commensurate with available computer resources. The *N*-acetyl-*N'*-methylglycinamide geometries are fully optimized (subject only to the two dihedral angle constraints) at the HF/3-21G level.^{25,26} This small, split-valence basis set²⁷ has been shown to behave reasonably well for geometry optimizations in comparison with the results obtained with

larger basis sets (6-31+G*)²⁸ and was adopted here only because of the large number of computations required to investigate chemical shifts over the full (ϕ, ψ) space. A grid with 30° intervals of the ϕ and ψ angles was used to give a total of 169 (13²) data points for the whole matrix, but only 84 data points were actually calculated, as the rest followed by symmetry.

All chemical-shielding calculations were based on the ab initio IGLO formulation of Kutzelnigg and Schindler.¹⁶ This method has been applied with good success to a large number of calculations of shielding for elements in the first and second rows and provides a satisfactory description of chemical shielding using modest basis sets. Qualitatively, this can be easily rationalized. The chemical shielding is very sensitive to the cancellation between large positive diamagnetic contributions σ^d and large negative paramagnetic contributions σ^p . Since diamagnetic terms can be calculated accurately even with small basis sets while the paramagnetic terms are exceedingly difficult to calculate, the cancellation between the two is most unfavorable. However, paramagnetic terms vanish if the origin is at the center of spherical orbitals. In the IGLO (and LORG²⁹) method localized MOs (LMOs) are associated with inner shells, bonding orbitals, and lone pairs. These are all roughly spherical, and the origins for the calculation of diamagnetic and paramagnetic terms are placed at the centroids of charge of the LMOs. This produces a substantial decrease in the magnitude of the paramagnetic-shielding magnitudes and, therefore, smaller cancellation errors between σ^d and σ^p .

There have been extensive studies of the basis set dependence of chemical shielding, and these are consistent with several IGLO calculations performed here at the double- ζ (DZ) level, e.g., basis set I is a (7,3/3) Huzinaga Gaussian lobe basis set³⁰ in the contraction (4111;21/21). Previous studies of ^{13}C chemical shifts^{17–21} showed that the conformational dependence is usually reproduced at this level. In the IGLO method larger basis sets almost always give better results in terms of absolute chemical shielding.¹⁶ For molecules of this size and the number of calculations involved, the use of larger basis sets is limited by the available computational facilities. The calculated isotropic ^{13}C shieldings σ , which are referenced to the bare nucleus, are converted to chemical shifts (δ) relative to TMS ($\sigma = 218.13$ ppm for the double- ζ basis set) for comparison with experimental results. All calculations were performed on a Convex C220 computer. Each IGLO calculation (DZ basis) required 2.5 h of CPU time. Geometry optimizations required 3–5 times longer. The ^{13}C chemical shift for the random coil geometry was estimated by Boltzmann averaging of the chemical shift profile $\delta(\phi, \psi)$ over the energy profile $E(\phi, \psi)$:

$$\langle \delta \rangle = \int \delta(\phi, \psi) e^{-E(\phi, \psi)/kT} d\phi d\psi / \int e^{-E(\phi, \psi)/kT} d\phi d\psi \quad (1)$$

The 3D surface plots, 2D projections of energy, and C_α chemical shifts were generated by a commercial plotting package which includes 2D and 3D spline algorithms (cubic or bicubic spline interpolation).³¹

III. Results and Discussion

A. Energy Surface of Gly Dipeptide in (ϕ, ψ) Space. Shown in Figure 2 is an energy surface plot of Gly dipeptide in (ϕ, ψ) space and its projection onto the (ϕ, ψ) plane. All energies are in kilocalories/mole relative to the lowest energy (−451.292 144 6 hartrees) for the (150°, 180°) conformation. No attempt was made to locate the various relative energy minima or transition states. The Gly dipeptide energy surface is similar to that for glycine dipeptide analogue (GDA), which was obtained with the same basis set by Head-Gordon and co-workers.²⁸ Existing energy maps for Gly dipeptide were based on the empirical conformational energy program for peptides (ECEPP) force field²² and the force field of Weiner et al.³² These force fields are widely used in conformational studies of peptides and proteins. The most obvious difference between the ECEPP and ab initio energy maps occurs

(15) For reviews of the various methods used in chemical shielding calculations, see: Jameson, C. J. *Nuclear Magnetic Resonance*; Specialist Periodical Reports 21; The Chemical Society: Burlington House, London, 1992; and previous chapters in this series. Webb, G. A. In *Nuclear Magnetic Shieldings and Molecular Structure*; Tossell, J. A., Ed.; Kluwer: Boston, 1993; pp 1–25.

(16) (a) Kutzelnigg, W. *Isr. J. Chem.* **1980**, *19*, 192–200. (b) Schindler, M.; Kutzelnigg, W. *J. Chem. Phys.* **1982**, *76*, 1919–1933. (c) For reviews of IGLO applications, see: Kutzelnigg, W. *J. Mol. Struct.* **1989**, *202*, 11–61. (d) Kutzelnigg, W.; Fleischer, U.; Schindler, M. *NMR Basic Principles and Progress*; Springer-Verlag: New York, 1990; Vol. 23, p 165. (e) Kutzelnigg, W.; van Wüllen, Ch.; Fleischer, U.; Franke, R.; Mourik, T. v. In *NMR Shieldings and Molecular Structure*; Tossell, J. A., Ed.; Kluwer Academic Publishers: Norwell, MA, 1993; pp 141–161.

(17) Barfield, M.; Yamamura, S. *J. Am. Chem. Soc.* **1990**, *112*, 4747–4758.

(18) Barfield, M. In *Nuclear Magnetic Shieldings and Molecular Structure*; Tossell, J. A., Ed.; Kluwer: Boston, 1993; pp 523–537.

(19) Barfield, M. *J. Am. Chem. Soc.* **1993**, *115*, 6916–6928.

(20) Jiao, D.; Barfield, M.; Combariza, J. E.; Hruby, V. J. *J. Am. Chem. Soc.* **1992**, *114*, 3639–3643.

(21) Jiao, D.; Barfield, M.; Hruby, V. J. *Magn. Reson. Chem.* **1993**, *31*, 75–79.

(22) Zimmerman, S. S.; Pottle, M. S.; Némethy, G.; Scheraga, H. A. *Macromolecules* **1977**, *10*, 1–9.

(23) Schindler, M.; Kutzelnigg, W. *J. Am. Chem. Soc.* **1983**, *105*, 1360–1370.

(24) Bühl, M.; Schleyer, P. v. R. *J. Am. Chem. Soc.* **1992**, *114*, 477–491.

(25) Hehre, W. J.; Radom, L.; Schleyer, P. v. R.; Pople, J. A. *Ab Initio Molecular Orbital Theory*; Wiley: New York, 1986.

(26) Frisch, M. J.; Head-Gordon, M.; Trucks, G. W.; Foresman, J. B.; Schlegel, H. B.; Raghavachari, K.; Robb, M.; Binkley, J. S.; Gonzalez, C.; Defrees, D. J.; Fox, D. J.; Whiteside, R. A.; Seeger, R.; Melius, C. F.; Baker, J.; Martin, R. L.; Kahn, L. R.; Stewart, J. J. P.; Topiol, S.; Pople, J. A. *Gaussian 90*, Revision I; Gaussian, Inc.: Pittsburgh, PA, 1990.

(27) Binkley, J. S.; Pople, J. A.; Hehre, W. J. *J. Am. Chem. Soc.* **1980**, *102*, 939–947.

(28) Head-Gordon, T.; Head-Gordon, M.; Frisch, M. J.; Brooks, C. L., III; Pople, J. A. *J. Am. Chem. Soc.* **1991**, *113*, 5989–5997.

(29) Hansen, Aa. E.; Bouman, T. D. *J. Chem. Phys.* **1985**, *82*, 5035–5047.

(30) Huzinaga, S. *Gaussian Basis Sets For Molecular Calculations*; Elsevier: New York, 1984.

(31) *Axum: Technical Graphics and Data Analysis*, 2nd ed.; TriMatrix, Inc.: Seattle, WA, 1992.

(32) Weiner, S. J.; Kollman, P. A.; Case, D. A.; Singh, U. C.; Ghio, C.; Alagona, G.; Profeta, S., Jr.; Weiner, P. *J. Am. Chem. Soc.* **1984**, *106*, 765–784.

(33) Barlow, D. J.; Thornton, J. M. *J. Mol. Biol.* **1988**, *201*, 601–619.

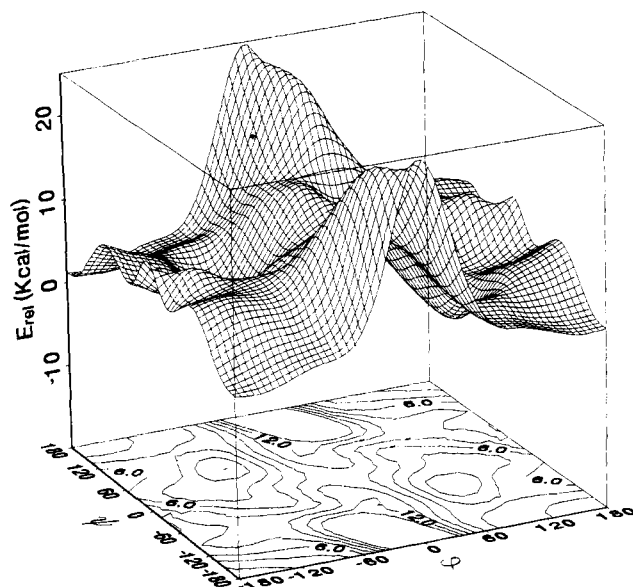


Figure 2. Calculated relative energies (HF/3-21G) of *N*-acetyl-*N'*-methylglycinamide plotted as a function of φ and ψ angles. The contour lines are separated by 2 kcal/mol.

in region A²² around $(-60^\circ, -50^\circ)$. This corresponds to the right-handed α -helical conformation in proteins and represents an obvious energy minimum which does not occur in the ab initio energy surface of Gly dipeptide or GDA.²⁸ Since lower energy for the α -helical protein conformations may be a result of solvent effects, a collective hydrogen-bonding effect, or a combination of both, they are not implicit in ab initio MO results for molecules in a vacuum. However, they must be implicit in the local force field parameters in order to produce results in agreement with experimental observations. The energy map for glycine dipeptide using the force field developed by Weiner and co-workers³² has more similarities with the one presented here, possibly because it is based on partial charges taken from ab initio Mulliken populations.

B. The ¹³C Chemical Shift of C α in Gly Dipeptide. Depicted in Figure 3 is a surface plot of the calculated ¹³C chemical shifts δ_C for the C α carbon of **1** as a function of φ and ψ angles. On this surface the chemical shift at highest field is 34.9 ppm for φ and ψ angles $(120^\circ, -150^\circ)/(-120^\circ, 150^\circ)$ and the one at lowest field occurs at 45.2 ppm $(0^\circ, 30^\circ)/(0^\circ, -30^\circ)$. This 10 ppm range is large enough to cover the δ_C variation (3.5–8.1 ppm)³ which has been observed in the solid-state NMR data for C α carbons of amino acid residues in peptides and proteins. In Table I the IGLO chemical shifts for the C α and C=O carbon for α_R -helix and antiparallel β -sheet conformations are compared with the experimental averages for glycylic residues. The chemical shifts for the carbonyl carbon are not correctly predicted.¹² A contributing factor may be the neglect of interresidue hydrogen bonding, but the inadequacies of small basis sets for geometry optimization and the chemical shifts for carbon bonded to N, O, and F heteroatoms^{18,19} should also be noted.

For the random coil geometry the calculated C α chemical shift of 39.1 ppm was obtained by numerical integration of eq 1 using the chemical shift and energy contour data. This value is 4.9 ppm smaller than the experimental average in Table I. More generally, the 4–5 ppm discrepancies between calculated and experimental chemical shifts for the C α carbon are typical at this level of theory.¹⁶ However, the relative chemical shift changes over different conformations are of primary interest here rather than the absolute chemical shifts as the differences are reproduced reasonably well even at the double- ζ level.^{17–21} The calculated ¹³C chemical shifts for the C α carbon in the α -helix region $(-48^\circ, -57^\circ)$ and in the β -sheet region $(-139^\circ, 135^\circ)$ are 2.3 ppm larger

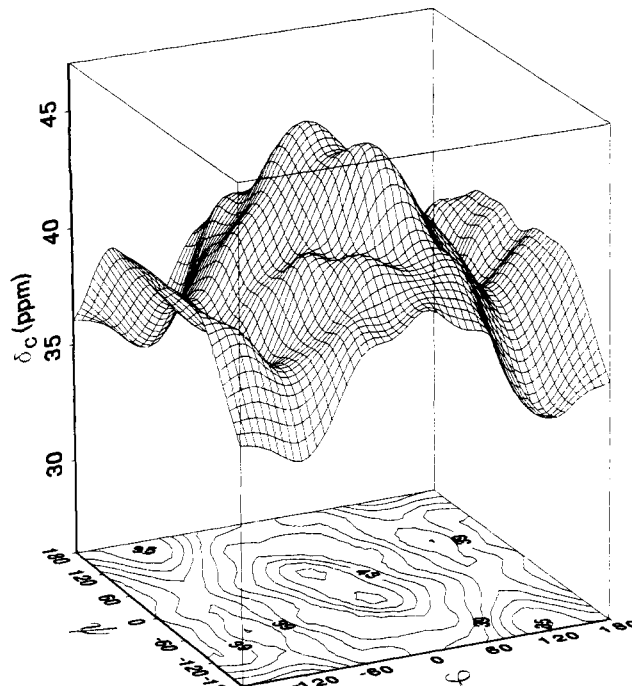


Figure 3. Calculated IGLO/DZ//HF/3-21G ¹³C chemical shifts of C α in *N*-acetyl-*N'*-methylglycinamide plotted versus φ and ψ angles. The contour lines are separated by 1 ppm.

Table I. Calculated C α ¹³C Chemical Shifts of Gly Dipeptide for Various Conformations Compared with Average Experimental Values in Glycyl Residues

conformation	φ (deg)	ψ (deg)	C α^a			C=O ^a	
			calc	WSR ^b	SB ^c	calc	WSR ^b
α_R -helix ^d	-48	-57	41.4	45.7	48.3 ^e	177.4	174.3
3 ₁₀ -helix ^d	-74	-4	40.3				
random coil			39.1	44.0	45.1		
parallel β -sheet ^d	-119	113	36.5				
antiparallel β -sheet ^f	-139	135	36.2	43.1 ^g	43.9 ^g	182.0	171.0
β -turn (type I), ^h $i+1$	-60	-30	40.7				
β -turn (type I), ^h $i+2$	-90	0	39.6				
β -turn (type II), ^h $i+1$	-60	120	41.2				
β -turn (type II), ^h $i+2$	80	0	40.1				
β -turn (type III), ^h $i+1$	-60	-30	40.7				
β -turn (type III), ^h $i+2$	-60	-30	40.7				

^a All values are given in parts per million. ^b These data from ref 7 are the mean value for glycylic residues in the various conformations. ^c These data from ref 6. ^d This notation conforms to that of Pauling et al.: Pauling, L.; Corey, R. B.; Branson, H. R. *Proc. Natl. Acad. Sci. U.S.A.* **1951**, *37*, 205–211. ^e These values were inferred from the secondary shift values and the random coil values in ref 6. ^f As defined in the following: Arnott, S.; Dover, S. D.; Elliott, E. *J. Mol. Biol.* **1967**, *30*, 209–212. ^g In ref 7 this chemical shift was assigned to β -strands; no distinction was made between parallel and antiparallel β -sheets. ^h This notation conforms to that of Lewis et al.: Lewis, P. N.; Momany, F. A.; Scheraga, H. A. *Biochim. Biophys. Acta* **1973**, *303*, 211–229.

and 2.9 ppm smaller than for the random coil, respectively. Considering the spread in the experimental data, these results are in reasonable agreement with data for glycylic residues,⁶ which average 3.2 and -1.2 ppm for α -helix and β -sheet secondary shifts, respectively. The β -sheet value is an average of secondary C α shifts, which range from -0.02 to -2.65 ppm. These values were included in the set of 119 α -helix residues and 126 β -sheet residues which was used by Spera and Bax to construct a histogram in which the average secondary shifts are 3.09 ± 1.00 and -1.48 ± 1.23 ppm for α -helix and β -sheet conformations, respectively.⁶ Wishart et al.⁷ also examined the average of glycine C α chemical shifts for a different set of molecules. These led to similar average values for the secondary shifts, i.e., 1.7 and -0.9 ppm in α -helix and β -sheet conformations, respectively.

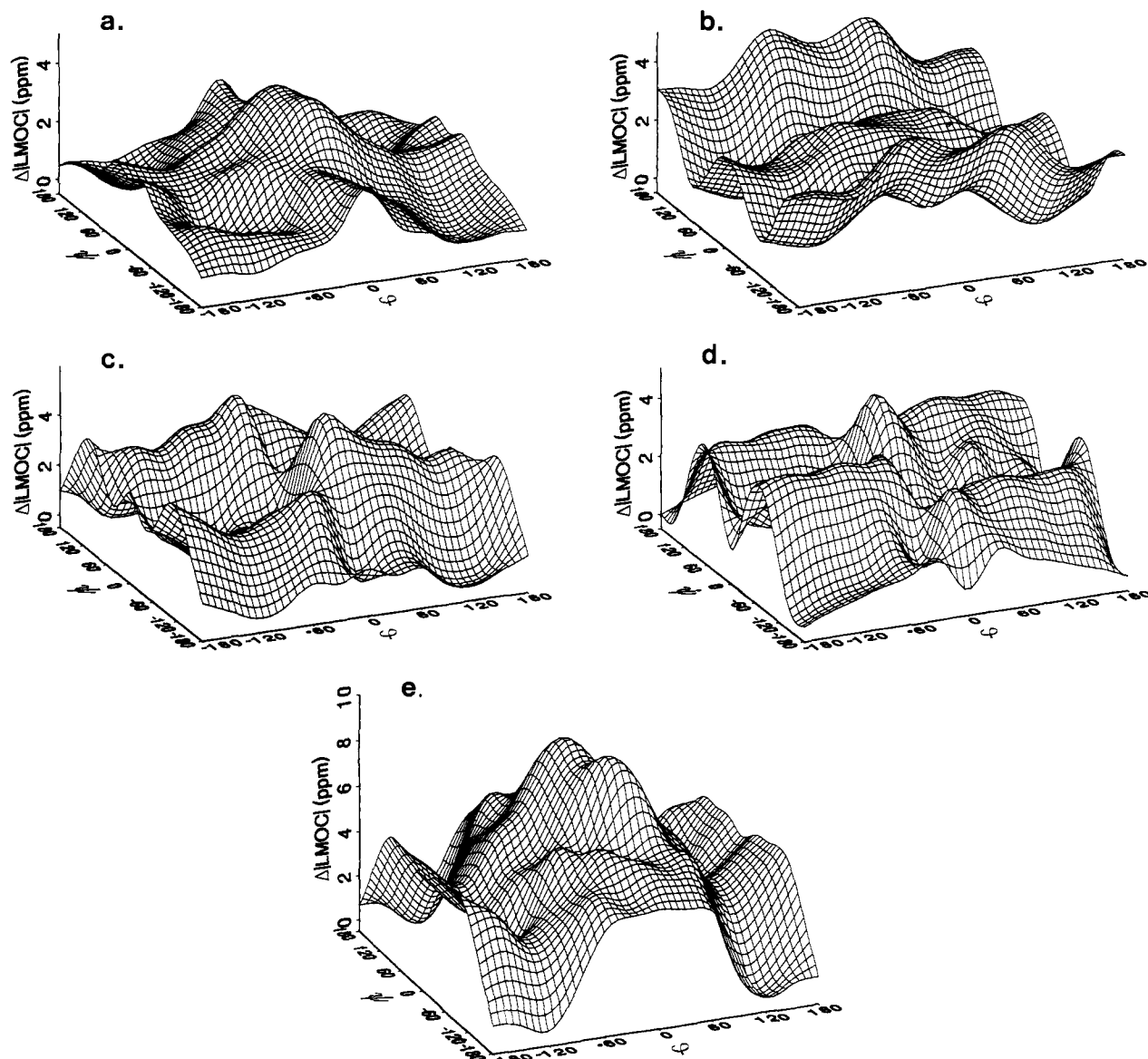


Figure 4. Calculated changes in the local MO contributions $\Delta|LMOC|$ from (a) the $C\alpha-C'$ bond, (b) the $C\alpha-N$ bond, (c) the $C\alpha-H_{proR}$ bond, (d) the $C\alpha-H_{proS}$ bond, and (e) a sum of all four bonds above plotted versus φ and ψ angles.

The calculated random coil chemical shift depends on the calculated energy profile, with the most important contributions arising from the low-energy regions. An alternative for comparison is the difference of 5.2 ppm between the calculated shifts for α -helix and β -sheet conformations. The two sets of experimental data for glycol residues in Table I show differences of 2.3 and 4.4 ppm. This difference becomes 4.6 ppm on including all the natural amino acids, excluding Cys and His.⁶ Larger chemical shift differences ($\Delta\delta_C$ up to 5.6 ppm) were observed for some amino acids⁷ such as Val and Arg. These differences between calculated and observed secondary ¹³C shifts are of the same order of magnitude as the uncertainties in the experimental data. For purposes of comparison, the average experimental data applied either to the same residue in different proteins or to different residues in the same protein. Chemical shifts for the $C\alpha$ carbon in the same amino acid residue and of the same conformational type can vary by 2–4 ppm. This deviation has been attributed to variations of protein secondary structure,⁶ since large deviations in the dihedral angles φ and ψ from the mean values of α -helices were observed even in the crystal structures of proteins³³ and peptides.³⁴ However, the calculated values in Table I correspond to the *standard* (φ, ψ) angles for these structures. These are probably not the same as the *averaged experimental ones*. The importance of chemical shift variations

around a particular set of (φ, ψ) angles can be easily seen from the $\delta(\varphi, \psi)$ map in Figure 3. For example, within the 32 and 20° ranges of standard deviations⁶ for φ and ψ angles in the β -sheet conformations,⁶ the calculated $C\alpha$ chemical shifts vary over a range of about 3 ppm. On the other hand, for ca. 10° standard deviations⁶ for the φ and ψ angles for the α -helix conformations,⁶ the calculated results show variations less than 1 ppm. These results are completely consistent with the larger error bars for β -sheet secondary shifts in comparison with α -helix secondary shifts.

The only clear distinctions among protein secondary structures, which are implicit in the experimental^{3,6,7} ¹³C NMR chemical shifts, are those for α -helix and β -sheet. It is apparent from the calculated $C\alpha$ chemical shift map (Figure 3) that variations of the $C\alpha$ chemical shifts induced by conformational changes are not limited to these two most common conformations. Other secondary structures, such as 3_{10} -helices and reverse turns, also induce changes in the $C\alpha$ chemical shifts. Calculated values for representative conformations are given in Table I. Although the conformationally induced chemical shifts were predicted for these

(34) Benedetti, E.; Blasio, B. D.; Pavone, V.; Pedone, C.; Santini, A.; Crisma, M.; Toniolo, C. In *Molecular Conformation And Biological Interactions*; Balaram, P., Ramaseshan, S., Eds.; Indian Academy of Sciences: Bangalore, India, 1991; pp 497–502.

folded structures, the magnitudes of δ_C variations are generally smaller than those observed between α -helices and β -sheets. All the δ_C 's for the reverse turns fall between the two limits imposed by α -helices and β -sheets, the two most common conformations in proteins. Because of the large deviations of the δ_C 's from the mean values observed in these two protein conformations,^{6,7} it is not clear that the predicted conformational dependence of the chemical shifts can be used to distinguish more precise conformational features beyond the general classification of helices and β -sheets. However, the calculated $C\alpha$ chemical shift map should prove to be helpful in interpreting the experimental data for small, conformationally constrained peptides, where reverse turn conformations are often observed.

In order to gain some insight into the conformational dependence of the $C\alpha$ chemical shifts, the contributions of each of the individual localized MOs to the total shielding (σ) of $C\alpha$ in Gly dipeptide **1** were examined. The major diamagnetic (positive) contribution to $\sigma(C\alpha)$ is 200.8 ppm from the inner-shell 1s orbital of the $C\alpha$ carbon. This number is approximately the same for the carbon atoms independent of the molecular conformation. The major negative contributions to the shielding arise from localized MOs (LMOs) associated with the four bonds at $C\alpha$, e.g., the $C\alpha-C'$, $C\alpha-N$, and two $C\alpha-H$ bonds. For the (180° , 180°) conformation the LMO contributions to the chemical shielding to $C\alpha$ are as follows (ppm): $C\alpha-C'$, -3.2; $C\alpha-N$, -3.7; $C\alpha-H_{\text{proR}}$, -2.9; $C\alpha-H_{\text{proS}}$, -2.9. These localized MO contributions not only account for a large percentage (>68%) of the total deshielding effect but also dominate the conformational dependence of $C\alpha$ chemical shifts. The sum over 22 other LMOs that are not directly connected to $C\alpha$ is only -6.1 ppm. To show the importance to the conformational effects of the localized MO contributions, the changes $\Delta|LMOC|$ for each of these four bonds are plotted in Figure 4a-d versus the φ and ψ angles. Absolute values are plotted to be consistent with the chemical shifts in Figure 3. Clearly, the overall conformational dependency of the $C\alpha$ chemical shifts over (φ , ψ) space cannot be attributed to the LMOC of any particular bond. Each of the localized MO contributions in Figure 4a-d varies by as much as 5 ppm over (φ , ψ) space. The sums of the four localized contributions in Figure 4e exhibit an approximate 10 ppm chemical shift variation and show the same general trends as the $C\alpha$ chemical shifts in Figure 3. However, the contributions from each of the LMOs are not the same for any two particular conformations such as α -helix and β -sheet. These LMO data are given in Table II. The localized MOs associated with the $C\alpha-C'$ bond and the $C\alpha-N$ bond produce the largest and the smallest contributions, respectively, to the chemical shift difference between the two conformations. Since the φ and ψ angles are measured about the $C\alpha-C'$ and $C\alpha-N$ bonds, respectively, it is tempting to relate the LMOC changes with the changes of electronic structures during rotation. A transition between the two conformations involves a change in the φ angle (91°) and a larger one (192°) in the ψ angle. It seems possible that a large change in the ψ angle leads to a correspondingly large change in the $C\alpha-C'$ bond LMO, which may influence the LMOC for the $C\alpha-C'$ bond.

Table II. Calculated ^{13}C Localized MO Contributions to the $C\alpha$ Chemical Shifts and Their Differences $\Delta\delta$ in α -Helix and β -Sheet Conformations^a

LMO	α -helix	β -sheet	$\Delta\delta$
$C\alpha-C'$	-5.0	-2.8	2.2
$C\alpha-N$	-2.7	-2.2	0.5
$C\alpha-N_{\text{proR}}$	-3.4	-2.4	1.0
$C\alpha-H_{\text{proS}}$	-6.5	-5.2	1.3
total	-17.6	-12.6	5.0

^a All values are given in parts per million. The differences in the last column are taken in the sense of the chemical shifts rather than chemical shielding.

IV. Conclusions

Complete energy and ^{13}C chemical shift maps were obtained at the IGLO/DZ//HF/3-21G level of ab initio MO theory for the model peptide *N*-acetyl-*N'*-methylglycinamide. These data were used to examine the relationship between ^{13}C chemical shifts and protein secondary structure. The predicted trends for the $C\alpha$ carbon agree with the available experimental data for α -helix and β -sheet conformations in peptides and proteins. Since the conformational dependence of $C\alpha$ chemical shifts can be explained largely in terms of changes in the electronic structure as the φ and ψ angles are varied, it is not necessary to invoke interresidue hydrogen-bonding effects. Although the chemical shift differences for other types of secondary structures are probably too small to distinguish precise conformational features in *proteins*, they should prove useful in interpreting the experimental data for *small, conformationally constrained peptides*, where reverse turn conformations are often observed.

In an attempt to sort out the conformationally induced changes of the electronic structure around $C\alpha$, the changes in the localized MO contributions, which are implicit in distributed-origins approaches, were examined. These provide somewhat more detail than the calculated chemical shifts, but they do not specify the electronic origins for observed effects. It is interesting to note that there is a rough correlation between the calculated LMO data and the associated bond lengths. Rather than the conformationally induced geometry changes being the responsible factor, it seems likely that the bond lengths and the LMO contributions have similar electronic origins. Conformational changes affect the electronic distributions, σ -bond orders, bond lengths, and paramagnetic contributions to the chemical shielding.

Acknowledgment. Thanks are extended to Professor W. Kutzelnigg and Dr. M. Schindler of the Ruhr-University Bochum for providing the IGLO88 program. We wish to thank Ms. Liping Gao for her technical assistance in compiling the IGLO program on the local Convex computer. The U.S. Public Health Service and The National Institute of Drug Abuse are gratefully acknowledged for grant support.

Supplementary Material Available: Table S1, giving all of the calculated shielding data and energies (2 pages). Ordering information is given on any current masthead page.